European Journal of Medicinal Chemistry 85 (2014) 228–234

Contents lists available at ScienceDirect

European Journal of Medicinal Chemistry

journal homepage: http://www.elsevier.com/locate/ejmech

Original article

Development of dual targeting inhibitors against aggregations of amyloid-β and tau protein

Shinichiro Fuse [a, *], Keisuke Matsumura [a], Yuki Fujita [b], Hachiro Sugimoto [b], Takashi Takahashi [c]

[a] Department of Applied Chemistry, Tokyo Institute of Technology, 2-12-1, Ookayama, Meguro-ku, Tokyo 152-8552, Japan
[b] Graduate School of Brain Science, Doshisha University, 4-1-1, Kizugawadai, Kizugawa-shi, Kyoto 619-0225, Japan
[c] Yokohama College of Pharmacy, 601, Matano-cho, Totsuka-ku, Yokohama-shi 245-0066, Japan

ARTICLE INFO

Article history:
Received 26 April 2014
Received in revised form
25 July 2014
Accepted 25 July 2014
Available online 26 July 2014

Keywords:
Alzheimer's disease
Amyloid-β
Tau
Aggregation
Suzuki–Miyaura coupling

ABSTRACT

Aggregations of both amyloid-β (Aβ) and hyper-phosphorylated tau proteins are recognized as key pathological manifestations of Alzheimer's disease (AD). Agents that inhibit both those forms of aggregation show promise as drug candidates. Seventeen oligo heteroaromatic compounds were rapidly synthesized via a one-pot, 3- or 4-component coupling procedure. Evaluations showed that compounds **E16** and **E18** were the most potent inhibitors of Aβ and tau aggregations (**E16**: IC_{50}s = 0.38, 0.29 μM against Aβ, tau, respectively, **E18**: IC_{50}s = 0.55, 0.30 μM against Aβ, tau, respectively).

1. Introduction

Thirty-five million people suffer from Alzheimer's disease (AD) worldwide, and the number of patients is estimated to triple by 2050. Moreover, in 2010 alone AD is estimated to have resulted in $604 billion in global healthcare expenditures [1,2]. Senile plaques (SPs) and neurofibrillary tangles (NFTs) are considered the key pathological hallmarks of AD. Aggregated amyloid-β (Aβ) and hyper-phosphorylated tau proteins are the main components of SPs and NFTs, respectively. Compelling evidence suggests that both Aβ and tau aggregations cause AD [1,3]. Several compounds, **1**–**6**, which targeted both the Aβ and tau aggregations (IC_{50}s < 3 μM against Aβ and tau) were reported (Fig. 1) [4]. All the compounds retained planer structures, and can be regarded as functional dyes. Among these dyes, only methylene blue (**3**) has reached the level of a phase III trial [2,5]. It should be noted that several dual targeting inhibitors against Aβ aggregation and acetyl/butyryl choline esterase have been reported recently [6,7].

Herein, we wish to report the rapid synthesis of **17** functional dyes via a one-pot, 3- or 4-component coupling procedure, and the evaluation of their inhibitory activity against the aggregations of Aβ and tau proteins. The dyes **E16** and **E18** showed high anti-aggregating activity (IC_{50}s against Aβ and tau < 1 μM), and they were more potent than methylene blue.

2. Results and discussion

Inspired by the fact that functional dyes **1**–**6** retained potent inhibitory activity against Aβ and tau protein aggregations, we briefly tested the inhibitory activities of thiophene-based organic dye **7** [8–12], which is a conventional donor-π-acceptor dye for dye-sensitized solar cells. The goal was to identify a new template for Alzheimer's drug discovery. In addition, the structure of **7** could be easily modified, which was needed in order to tune its properties for drug development. Surprisingly, dye **7** showed a level of inhibitory activity that compared favorably to those of methylene blue (Fig. 2). Thus, we decided to synthesize a small library based on **7**.

We have reported library synthesis based on Suzuki–Miyaura coupling [13–15]. Gruttadauria and co-workers have demonstrated a one-pot, 3-component coupling (SM coupling/Knoevenagel condensation) [16]. In our study, a one-pot, 3- or 4-component coupling (SM coupling/SM coupling or SM coupling/SM coupling/Knoevenagel condensation) approach was employed for the library

* Corresponding author.
E-mail address: sfuse@apc.titech.ac.jp (S. Fuse).

http://dx.doi.org/10.1016/j.ejmech.2014.07.095
0223-5234/

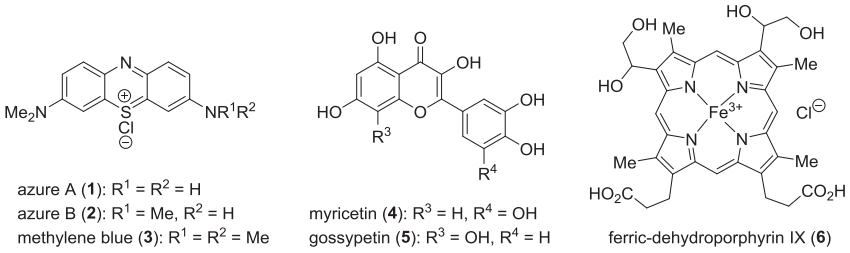

Fig. 1. (a) Structures of azure A (**1**), azure B (**2**), methylene blue (**3**), myricetin (**4**), gossypetin (**5**), and ferric-dehydroporphyrin IX (**6**), which retained potent inhibitory activities against Aβ (IC_{50}s: **1**; 0.4 μM, **2**; 0.3 μM, **3**; 2.3 μM, **4**; 0.9 μM, **5**; 1.3 μM, **6**; 0.2 μM) and tau protein (IC_{50}s: **1**; 2.6 μM, **2**; 1.9 μM, **3**; 1.9 μM, **4**; 1.2 μM, **5**; 2.0 μM, **6**; 1.4 μM) aggregations.

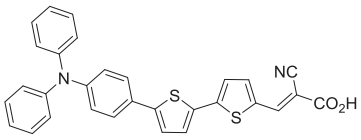

Fig. 2. (a) Structure of the thiophene-based organic dye **7**, and its inhibitory activities against Aβ and tau proteins aggregations.

synthesis, as shown in Fig. 3. We planned to couple donor block **A** with the aromatic scaffold **B** at first because the C–Br bond of the first coupling product would be less reactive compared with the corresponding C–Br bond of the aromatic scaffold **B**, and, therefore, an undesired overreaction affording an **A-B-A** compound would be suppressed. The following SM coupling and Knoevenagel condensation would afford the desired dyes.

The reaction conditions for the one-pot, 4-component coupling of **A1**, **B1**, **C**, and **D1** were explored (Table 1). Combinations of bases (K_3PO_4 and Na_2CO_3), Pd catalysts {$Pd(PPh_3)_4$ [17] and $Pd_2(dba)_3$ [18]}, and phosphine ligands {Xantphos [19] and $[(t\text{-}Bu)_3PH]BF_4$ [20]} were examined. It seemed that the selection of a base was important in this reaction. The use of K_3PO_4 afforded better yields (entries 1, 3, and 5) compared with the use of Na_2CO_3 (entries 2, 4, and 6), probably due to the better solubility of K_3PO_4 against the toluene/EtOH solvent. The use of an electron-rich and bulky ligand, $[(t\text{-}Bu)_3PH]BF_4$ for the first SM coupling resulted in low yields (entries 5 and 6) due to the overreaction of **A1** with the first coupling product, **A1**-**B1**, to generate the undesired **A1**-**B1**-**A1**. The combination of $Pd_2(dba)_3$ and Xantphos as a Pd catalyst and a phosphine ligand for the first SM coupling afforded the best result (entry 3). The conditions shown in entry 1 also afforded results comparable to the best combination (entry 1) (Table 1).

The building blocks were coupled using the developed one-pot conditions (Table 2). As a result, 8 compounds **E3**, **E5**, **E7**, **E10**, **E11**, **E13**, **E17**, and **E18** were successfully synthesized from the one-pot, 4-component coupling procedure, and 6 aldehydes, **E2**, **E6**, **E9**, **E12**, **E16**, **E19** were synthesized from the one-pot, 3-component coupling procedure. In regard to the *E*- and *Z*-geometries of alkenes generated by Knoevenagel condensation between aldehydes and cyanoacetamide (**D2**), ^1H NMR analysis revealed that the products retained the *E*-alkene form [21,22]. Unexpectedly, **E4**, **E8**, **E14**, and **E15** could not be obtained from the one-pot procedure. In the case of **E4**, the building block **D3** was not soluble against the toluene/EtOH solvent that was utilized for the one-pot procedure;

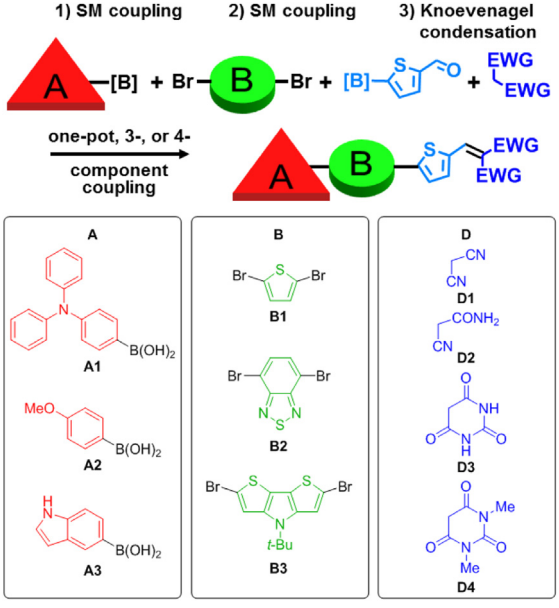

Fig. 3. Synthesis of structurally diverse organic dyes via a one-pot, 3- or 4-component coupling (SM coupling/SM coupling or SM coupling/SM coupling/Knoevenagel condensation) approach.

Table 1
One-pot, 4-component coupling of **A1**, **B1**, **C**, and **D1**.

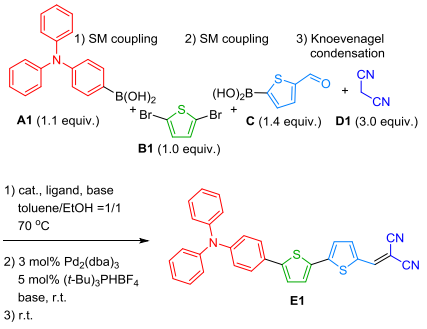

Entry	Pd cat.	Ligand	Base	Yield[d]
1	$Pd(PPh_3)_4$[a]	–	K_3PO_4	38%
2	$Pd(PPh_3)_4$[a]	–	Na_2CO_3	9%
3	$Pd_2(dba)_3$[b]	Xantphos[c]	K_3PO_4	40%
4	$Pd_2(dba)_3$[b]	Xantphos[c]	Na_2CO_3	12%
5	$Pd_2(dba)_3$[b]	$[(t\text{-}Bu)_3PH]BF_4$[c]	K_3PO_4	6%
6	$Pd_2(dba)_3$[b]	$[(t\text{-}Bu)_3PH]BF_4$[c]	Na_2CO_3	6%

[a] 1 mol%.
[b] 0.5 mol%.
[c] 2 mol%.
[d] Isolated yield (one-pot, 3-step yield based on **B1**).

thus, Knoevenagel condensation did not proceed. Therefore, Knoevenagel condensation of the isolated aldehyde **E2** (one-pot, 3-component coupling product) with the building block **D3** under AcOH solvent conditions (**D3** was soluble against AcOH) was carried out to obtain the desired compound **E4** (95% yield). In the case of **E8**, the desired product was obtained with multiple undesired compounds, and the purification was difficult due to the insufficient solubility of **E8**. Therefore, Knoevenagel condensation of the isolated aldehyde **E6** was carried out to obtain a purer form of **E8**. As expected, simple short-pad column chromatography of the Knoevenagel condensation product afforded **E8** in a 53% yield. In the cases of **E14** and **E15**, the desired products could not be purified due to their poor solubility.

The anti-aggregating activity against the Aβ [23, 24] and the tau [25] of 17 synthesized organic dyes was briefly tested (Table 3). As a result, 5 dyes, **E2**, **E3**, **E13**, **E16**, and **E18**, exerted IC_{50}s of less than 10 μM, whereas the 5 dyes, **E4**–**E8** retained **D3**, **D4**, or **B2** building blocks and showed no potent anti-aggregating activity against Aβ and tau proteins (IC_{50}s > 10 μM). This detrimental effect of the building blocks **D3**, **D4**, and **B2** on the inhibitory activities might be attributable to a decrease in molecular planarity, because these building blocks tended to twist the π-conjugated plane in order to reduce steric repulsions between adjacent aromatic rings. In terms of inhibitory activity against tau aggregation, 2 dyes, **E16** and **E18**, retained **A2** and **B3** and 1 dye, **E19**, retained an **A3** building block, and these exerted high inhibitory activity (inhibitory rate of **E16**: 74% at 1 μM, IC_{50} of **E18** = 1.4 μM, IC_{50} of **E19** = 1.6 μM), whereas the remaining 14 dyes showed no potent anti-aggregating activity against tau proteins (IC_{50}s > 10 μM). It is interesting that active dyes **E16**, **E18**, and **E19** retained pyrrole and bithiophene moieties. Three dyes **E2**, **E3**, and **E13** showed inhibitory activity only against Aβ aggregation. Among the 17 synthesized dyes, only 2, **E16** and **E18**, retained potent inhibitory activity against both Aβ and tau aggregations. All the structural components in the dyes **E16** and **E18** seemed to be important for anti-aggregating activity against both Aβ and tau: structural alterations of the aldehyde and the cyanoacryl amide to malononitrile (**E16** to **E17**, **E18** to **E17**), and structural alterations of the 4-methoxy benzene to triphenyl amine (**E16** to **E9**, **E18** to **E11**) decreased the anti-aggregating activities of **E16** and **E18** against both Aβ and tau. In addition, structural alteration of *tert*-butyl dithienopyrrole in **E16** to thiophene (**E16** to **E12**) also decreased the anti-aggregating activities against both Aβ and tau.

The IC_{50}s of the most active compounds, **E16** and **E18**, were carefully determined (Table 4). The IC_{50}s of methylene blue (**3**) and dye **7** were also determined to be positive controls. To our delight, both dyes **E16** and **E18** retained a level of anti-Aβ aggregation activity that compared favorably to those of methylene blue (**3**) and dye **7**. Moreover, both dyes **E16** and **E18** exerted approximately 10 times more potent anti-tau aggregation activity. As far as we could ascertain, dyes **E16** and **E18** are the first compounds to show submicromolar IC_{50}s against the aggregation of both Aβ and tau protein.

Table 2
One-pot, 3- or 4-component coupling for the synthesis of functional dyes.

Entry	Substrate			Product	Yield
	A	**B**	**D**	**E**	
1	**A1**	**B1**	–	**E2**	55%[a]
2	**A1**	**B1**	**D2**	**E3**	29%[b]
3	**A1**	**B1**	**D3**	**E4**	(95%)[c]
4	**A1**	**B1**	**D4**	**E5**	23%[b]
5	**A1**	**B2**	–	**E6**	74%[a]
6	**A1**	**B2**	**D1**	**E7**	56%[b]
7	**A1**	**B2**	**D2**	**E8**	(53%)[d]
8	**A1**	**B3**	–	**E9**	28%[a]
9	**A1**	**B3**	**D1**	**E10**	30%[b]
10	**A1**	**B3**	**D2**	**E11**	27%[b]
11	**A2**	**B1**	–	**E12**	48%[a]
12	**A2**	**B1**	**D1**	**E13**	22%[b]
13	**A2**	**B1**	**D2**	**E14**	–[e]
14	**A2**	**B2**	–	**E15**	–[e]
15	**A2**	**B3**	–	**E16**	34%[a]
16	**A2**	**B3**	**D1**	**E17**	34%[b]
17	**A2**	**B3**	**D2**	**E18**	11%[b]
18	**A3**	**B1**	–	**E19**	42%[a]

[a] Isolated yields of one-pot, 3-component SM coupling based on **B**.
[b] Isolated yields of one-pot, 4-component coupling based on **B**.
[c] The building block, **D3** was poorly soluble against toluene/EtOH solvent, therefore, the desired product, **E4**, was not obtained via one-pot, 4-component coupling. **E4** was synthesized from Knoevenagel condensation of the isolated **E2** and the building block **D3** (one-pot, 3-component coupling product) under AcOH solvent conditions. The yield of Knoevenagel condensation is shown in parenthesis.
[d] The desired product of one-pot, 4-component coupling, **E8**, could not be separated from the undesired products due to its insufficient solubility. Knoevenagel condensation (piperidine, CH_2Cl_2/MeCN = 2/1, 40 °C) of the isolated **E6** and the following short-pad column chromatography afforded the desired **E8**. The yield of Knoevenagel condensation is shown in parenthesis.
[e] The desired products could not be purified due to their poor solubility.

3. Conclusion

In summary, we demonstrated the rapid synthesis of 17 structurally-diverse, organic dyes via our originally developed one-pot, 3- or 4-component coupling procedure (SM coupling/SM coupling or SM coupling/SM coupling/Knoevenagel condensation). Anti-aggregating activities of the synthesized dyes were evaluated, and 2 compounds, **E16** and **E18**, showed sub-micromolar IC_{50}s against the aggregation of both Aβ and tau proteins. As far as we could ascertain, these compounds are the first to demonstrate this quality. Thus, we have successfully identified a totally new template for Alzheimer's drug discovery.

Although we tried to measure the log Ps of the most active dyes **E16** and **E18**, they could not be determined due to their very poor solubility against water. It is important to improve the water solubility of these dyes by introducing hydrophilic groups to further develop them for use as an Alzheimer's drug.

4. Experimental

4.1. Chemistry

NMR spectra were recorded on a JEOL Model ECP-400 (400 MHz for ^1H, 100 MHz for ^{13}C) instrument for the indicated solvent. Chemical shifts were reported in units of parts per million (ppm) relative to the signal for internal tetramethylsilane (0.00 ppm for ^1H) for solutions in $CDCl_3$. The ^1H NMR spectral data were reported as follows: $CDCl_3$ (7.26 ppm), DMSO-d_6 (2.49 ppm). ^{13}C NMR spectral data were reported as follows: $CDCl_3$ (77.0 ppm), DMSO-d_6 (39.5 ppm). Multiplicities were reported using the following abbreviations: s, singlet; d, doublet; dd, doublet of doublets; t, triplet; m, multiplet; br. broad; *J*, coupling constants in Hertz. The IR spectra were recorded on a Perkin Elmer Spectrum One FT-IR spectrophotometer. Only the strongest and/or structurally important absorption data are reported as the IR data given in cm^{-1}. All reactions were monitored by thin-layer chromatography carried out on 0.2 mm E. Merck silica gel plates (60F-254) with UV light, visualized by *p*-anisaldehyde solution, ceric sulfate or 10% ethanolic phosphomolybdic acid. Column chromatography was performed on Kanto Chemical Co. silica gel 60 (0.063–0.200 mm). ESI-TOF Mass spectra were measured using a Waters LCT Premier™ XE. The HRMS (ESI-TOF) was calibrated using leucine enkephalin.

Table 3
Inhibitory activities of the synthesized 17 compounds against Aβ and tau aggregations.

Entry	Compound	Structure	IC_{50} [μM] against A	IC_{50} [μM] against tau
1	**E1**	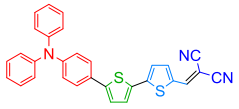	>10 43% at 10 μM[a]	>10 14% at 10 μM[a]
2	**E2**	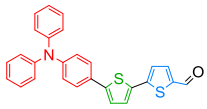	7.1	>10 12% at 10 μM[a]
3	**E3**	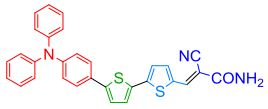	1.5	>10 29% at 10 μM[a]
4	**E4**	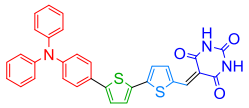	>10 0% at 10 μM[a]	>10 12% at 10 μM[a]
5	**E5**	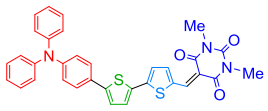	>10 18% at 10 μM[a]	>10 7% at 0 μM[a]
6	**E6**	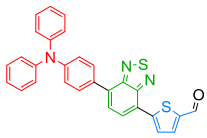	>10 44% at 10 μM[a]	>10 11% at 0 μM[a]
7	**E7**	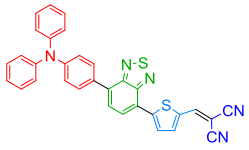	>10 30% at 10 μM[a]	>10 15% at 0 μM[a]
8	**E8**	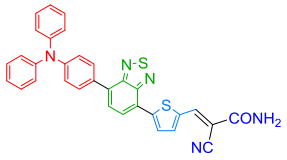	>10 46% at 10 μM[a]	>10 24% at 10 μM[a]
9	**E9**	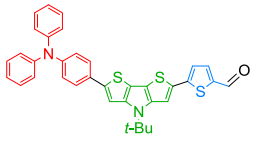	>10 36% at 10 μM[a]	>10 15% at 10 μM[a]
10	**E10**	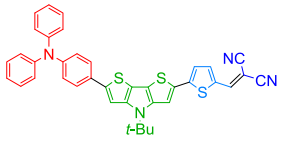	>10 16% at 10 μM[a]	>10 18% at 10 μM[a]
11	**E11**	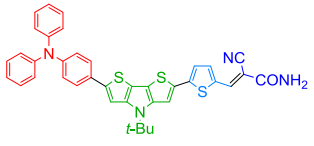	>10 36% at 10 μM[a]	>10 33% at 10 μM[a]

Table 3 (*continued*)

Entry	Compound	Structure	IC_{50} [μM] against A	IC_{50} [μM] against tau
12	**E12**	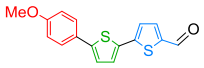	>10 0% at 10 μM[a]	>10 18% at 10 μM[a]
13	**E13**	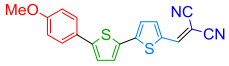	<1 78% at 1 μM[a]	>10 28% at 10 μM[a]
14	**E16**	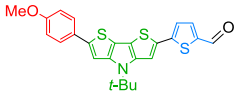	<1 61% at 1 μM[a]	<1 74% at 1 μM[a]
15	**E17**	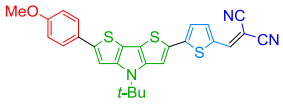	>10 18% at 10 μM[a]	>10 27% at 10 μM[a]
16	**E18**	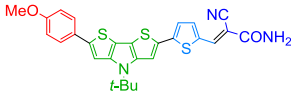	1.8	1.4
17	**E19**	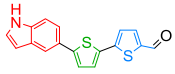	>10 46% at 10 μM[a]	1.6
18	**7**	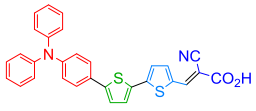	<1 82% at 1 μM[a]	1.7
19	**Methylene blue (3)**		0.9	2.2

[a] Inhibitory rates at indicated concentrations of compounds.

4.2. General procedure for one-pot, 3-component coupling (SM coupling/SM coupling)

A solution of **A** block (1.10 equiv.), **B** block (1.00 equiv.), $Pd(PPh_3)_4$ (0.0100 equiv.), and K_3PO_4 (2.00 equiv.) in a mixture of toluene (5.00 mL/mmol) and EtOH (5.00 mL/mmol) was degassed with argon. After being stirred at 70 °C for 8–10 h (monitored by TLC), the mixture was cooled to room temperature, then 5-formylthiophenyl-2-boronic acid (**C**) (1.40 equiv.), $Pd_2(dba)_3$ (0.0300 equiv.), $[(t\text{-Bu})_3PH]BF_4$ (0.0500 equiv.), and K_3PO_4 (2.00 equiv.) were added. After being stirred at room temperature for 2–10 h (monitored by TLC), the mixture was poured into water, and the aqueous layer was extracted with two portions of chloroform. The organic layer was dried over $MgSO_4$, and evaporated *in vacuo*. The residue was purified by column chromatography on silica gel with toluene and further purified by recrystallization with chloroform:hexane to give the product.

4.2.1. Compound ***E2*** [8,10,11,26–30]

Orange solid; yield 55%; Mp 137–138 °C; ^1H NMR (400 MHz, $CDCl_3$): δ 9.84 (s, 1H), 7.64 (d, 1H, $J = 4.4$ Hz), 7.44 (d, 2H, $J = 8.7$ Hz), 7.30–7.24 (m, 5H), 7.22 (d, 1H, $J = 4.4$ Hz), 7.15 (d, 1H, $J = 4.4$ Hz), 7.12 (d, 4H, $J = 8.7$ Hz), 7.07–7.04 (m, 4H); ^{13}C NMR (100 MHz,

Table 4
IC_{50}s of compounds **E16** and **E18** against Aβ and tau proteins aggregation.

Entry	Compound	IC_{50} [μM][a] against A	IC_{50} [μM][a] against tau
1	**E16**	0.38	0.29
2	**E18**	0.55	0.30
3	**7**	0.41	3.6
4	**3**	0.55	2.4

[a] Average values from two independent experiments.

$CDCl_3$): δ 182.3, 148.0, 147.4, 147.2, 146.2, 141.2, 137.4, 134.0, 129.4, 127.2, 127.0, 126.6, 124.8, 123.7, 123.4, 123.2, 123.1; FT-IR (neat) 3065, 1736, 1661, 1592, 1522, 1490, 1455, 1327, 1282, 1229, 1050, 882, 830, 791, 753, 696, 528, 478 cm^{-1}; HRMS (ESI-TOF): calcd. for $C_{27}H_{20}NOS_2$ $[M+H]^+$ 438.0986 found 438.0986.

4.2.2. Compound ***E6*** [31,32]

Red solid; yield 74%; Mp 169–172 °C; ^1H NMR (400 MHz, $CDCl_3$): δ 9.98 (s, 1H), 8.22 (d, 1H, $J = 3.9$ Hz), 8.05 (d, 1H, $J = 7.8$ Hz), 7.89 (d, 2H, $J = 8.7$ Hz), 7.86 (d, 1H, $J = 3.9$ Hz), 7.75 (d, 1H, $J = 7.8$ Hz), 7.30 (dd, 4H, $J = 8.8$, 7.3 Hz), 7.22–7.18 (m, 6H), 7.09 (t, 2H, $J = 7.3$ Hz); ^{13}C NMR (100 MHz, $CDCl_3$): δ 182.9, 153.8, 152.7, 148.9, 148.6, 147.3, 143.3, 136.7, 134.6, 130.0, 129.9, 129.4, 127.8, 127.6, 126.7, 125.1, 124.2, 123.6, 122.4; FT-IR (neat): 3034, 2317, 1664, 1591, 1510, 1487, 1443, 1331, 1283, 1222, 1050, 881, 818, 754, 697, 668, 623, 513 cm^{-1}; HRMS (ESI-TOF): calcd. for $C_{29}H_{20}N_3OS_2$ $[M+H]^+$ 490.1048, found 490.1021.

4.2.3. Compound ***E9***

Red solid; yield 28%; Mp 207–210 °C; ^1H NMR (400 MHz, $CDCl_3$): δ 9.83 (s, 1H), 7.65 (d, 1H, $J = 3.8$ Hz), 7.50–7.48 (m, 3H), 7.34 (s, 1H), 7.29–7.26 (m, 4H), 7.22 (d, 1H, $J = 3.8$ Hz), 7.13 (d, 4H, $J = 7.8$ Hz), 7.09–7.03 (m, 4H), 1.84 (s, 9H); ^{13}C NMR (100 MHz, $CDCl_3$): δ 182.1, 149.2, 147.4, 145.1, 143.0, 142.7, 140.5, 137.6, 131.6, 129.3, 129.2, 126.4, 124.6, 123.6, 123.2, 122.9, 118.2, 115.1, 113.5, 109.9, 58.4, 30.7; FT-IR (neat): 2983, 1658, 1591, 1505, 1494, 1420, 1370, 1281, 1229, 1094, 1051, 798, 753, 697, 513 cm^{-1}; HRMS (ESI-TOF): calcd. for $C_{35}H_{29}N_2OS_3$ $[M+H]^+$ 589.1442, found 589.1491.

4.2.4. Compound ***E12***

Yellow solid; yield 48%; Mp 166–169 °C; ^1H NMR (400 MHz, $CDCl_3$): δ 9.85 (s, 1H), 7.66 (d, 1H, $J = 3.8$ Hz), 7.54 (d, 2H, $J = 8.7$ Hz), 7.31 (d, 1H, $J = 3.9$ Hz), 7.23 (d, 1H, $J = 3.8$ Hz), 7.15 (d, 1H, $J = 3.9$ Hz), 6.93 (d, 2H, $J = 8.7$ Hz), 3.85 (s, 3H); ^{13}C NMR (100 MHz, $CDCl_3$): δ 182.4, 159.8, 147.4, 146.3, 141.3, 137.4, 134.1, 127.2, 126.3, 123.7, 123.1, 114.5, 55.4; FT-IR (neat): 2934, 1660, 1607, 1506, 1444, 1286, 1260, 1179, 1114, 1027, 880, 831, 795, 752, 482 cm^{-1}; HRMS (ESI-TOF): calcd. for $C_{16}H_{13}O_2S_2$ $[M+H]^+$ 301.0357, found 301.0338.

4.2.5. Compound ***E16***

Orange solid; yield 34%; Mp 225–227 °C; ^1H NMR (400 MHz, $CDCl_3$): δ 9.84 (s, 1H), 7.66 (d, 1H, $J = 4.4$ Hz), 7.57 (d, 2H, $J = 8.8$ Hz), 7.49 (s, 1H), 7.33 (s, 1H), 7.23 (d, 1H, $J = 4.4$ Hz), 6.94 (d, 2H, $J = 8.8$ Hz), 3.85 (s, 3H), 1.85 (s, 9H); ^{13}C NMR (100 MHz, $CDCl_3$): δ 182.1, 159.4, 149.2, 145.1, 143.1, 142.6, 140.5, 137.5, 131.5, 128.1, 126.9, 122.9, 118.1, 115.0, 114.4, 113.5, 109.9, 58.4, 55.4, 30.7; FT-IR (neat): 2984, 1659, 1526, 1506, 1469, 1421, 1370, 1293, 1230, 1180, 1056, 1028, 831, 805, 752, 662, 511 cm^{-1}; HRMS (ESI-TOF): calcd. for $C_{24}H_{22}NO_2S_3$ $[M+H]^+$ 452.0813, found 452.0825.

4.2.6. Compound ***E19***

Yellow solid; yield 42%; Mp 190–193 °C; ^1H NMR (400 MHz, DMSO-d_6): δ 11.27 (s, 1H), 9.86 (s, 1H), 7.96 (d, 1H, $J = 3.9$ Hz), 7.89 (s, 1H), 7.55 (d, 1H, $J = 3.9$ Hz), 7.49–7.40 (m, 5H), 6.49 (br-s, 1H); ^{13}C NMR (100 MHz, DMSO-d_6): δ 183.5, 147.8, 146.0, 140.6, 139.2, 136.0, 132.5, 128.2, 128.1, 126.7, 124.4, 124.0, 123.3, 119.3, 117.3, 112.1, 101.7; FT-IR (neat): 3272, 1633, 1438, 1382, 1317, 1232, 1105, 1066, 1047, 881, 782, 767, 680, 576, 482 cm^{-1}; HRMS (ESI-TOF): calcd. for $C_{17}H_{12}NOS_2$ $[M+H]^+$ 310.0360, found 310.0341.

4.3. General procedure for one-pot, 4-component coupling (SM coupling/SM coupling/Knoevenagel condensation)

A solution of **A** block (1.00 equiv.), **B** block (1.10 equiv.), $Pd(PPh_3)_4$ (0.0100 equiv.), and K_3PO_4 (2.00 equiv.) in a mixture of toluene (5.00 mL/mmol) and EtOH (5.00 mL/mmol) was degassed with argon. After being stirred at 70 °C for 8–10 h (monitored by TLC), the mixture was cooled to room temperature, then 5-formylthiophenyl-2-boronic acid (**C**) (1.40 equiv.), $Pd_2(dba)_3$ (0.0300 equiv.), $[(t\text{-}Bu)_3PH]BF_4$ (0.0500 equiv.), and K_3PO_4 (2.00 equiv.) were added. After being stirred at room temperature for 2–10 h (monitored by TLC), **D** block (malononitrile, cyanoacrylamide, or *N*,*N*-dimethylbarbituric acid, 3.00 equiv.) was added. After being stirred at room temperature for 1–2 h (malononitrile or *N*,*N*-dimethylbarbituric acid) or 5–6 h (cyanoacetamide), the mixture was poured into water, and the aqueous layer was extracted with two portions of chloroform. The organic layer was dried over $MgSO_4$, and evaporated *in vacuo*. The residue was purified by column chromatography on silica gel with toluene and further purified by recrystallization with chloroform:hexane to give the product.

4.3.1. Compound ***E1*** [27,29]

Black solid; yield 38%; Mp 182–184 °C; ^1H NMR (400 MHz, $CDCl_3$): δ 7.74 (s, 1H), 7.62 (d, 1H, $J = 4.4$ Hz), 7.46 (d, 2H, $J = 8.8$ Hz), 7.40 (d, 1H, $J = 3.9$ Hz), 7.31–7.26 (m, 5H), 7.21 (d, 1H, $J = 3.9$ Hz), 7.13 (d, 4H, $J = 7.7$ Hz), 7.10–7.05 (m, 4H); ^{13}C NMR (100 MHz, $CDCl_3$): δ 149.8, 149.7, 148.6, 148.0, 147.3, 139.9, 133.2, 129.5, 128.4, 126.8, 126.7, 125.1, 124.1, 123.7, 123.5, 122.9, 114.3, 113.5, 75.9; FT-IR (solid): 3022, 2924, 2855, 2215, 1567, 1534, 1485, 1439, 1322, 1230, 1143, 1055, 935, 806, 754, 727, 694, 516 cm^{-1}; HRMS (ESI-TOF): calcd. for $C_{30}H_{20}N_3S_2$ $[M+H]^+$ 486.1099, found 486.1098.

4.3.2. Compound ***E3***

Red solid; yield 29%; Mp 229–230 °C; ^1H NMR (400 MHz, DMSO-d_6): δ 8.34 (s, 1H), 7.82 (d, 1H, $J = 3.9$ Hz), 7.76 (br-s, 1H), 7.66 (br-s, 1H), 7.62 (d, 2H, $J = 8.8$ Hz), 7.57 (d, 1H, $J = 3.9$ Hz), 7.53 (d, 1H, $J = 3.9$ Hz), 7.47 (d, 1H, $J = 3.9$ Hz), 7.34 (dd, 4H, $J = 8.6$, 7.3 Hz), 7.11–7.06 (m, 6H), 6.96 (d, 2H, $J = 8.8$ Hz); ^{13}C NMR (100 MHz, DMSO-d_6): δ 162.6, 147.5, 146.6, 145.0, 144.3, 143.2, 139.9, 133.9, 133.2, 129.7, 128.0, 126.6, 126.4, 124.6, 124.2, 123.7, 122.5, 116.9, 100.7; FT-IR (solid): 3347, 3189, 3064, 2207, 1735, 1673, 1577, 1542, 1490, 1445, 1377, 1282, 1052, 794, 754, 696, 517 cm^{-1}; HRMS (ESI-TOF): calcd. for $C_{30}H_{22}N_3OS_2$ $[M+H]^+$ 504.1204, found 504.1184.

4.3.3. Compound ***E5***

This compound was purified by column chromatography on silica gel with 90:10 toluene:ethyl acetate and further purified by recrystallization with toluene:hexane.

Dark red solid; Mp 253–254 °C; ^1H NMR (400 MHz, $CDCl_3$): δ 8.59 (s, 1H), 7.75 (d, 1H, $J = 3.9$ Hz), 7.49–7.45 (m, 3H), 7.33–7.27 (m, 5H), 7.20 (d, 1H, $J = 3.9$ Hz), 7.13 (d, 4H, $J = 7.3$ Hz), 7.09–7.05 (m, 4H), 3.43 (s, 3H), 3.40 (s, 3H); ^{13}C NMR (100 MHz, $CDCl_3$): δ 162.8, 162.1, 154.0, 151.4, 148.3, 148.1, 147.5, 147.2, 147.1, 135.2, 134.3, 129.4, 128.2, 126.9, 126.6, 124.9, 124.2, 123.6, 123.5, 122.9, 108.5, 28.8, 28.1; FT-IR (solid): 2924, 1724, 1665, 1590, 1563, 1538, 1489, 1421, 1352, 1324, 1286, 1158, 1079, 969, 828, 796, 752, 697, 522, 493 cm^{-1}; HRMS (ESI-TOF): calcd. for $C_{33}H_{26}N_3O_3S_2$ $[M+H]^+$ 576.1416, found 576.1409.

4.3.4. Compound **E7**

Black solid; yield 56%; Mp 246–250 °C; ^{1}H NMR (400 MHz, $CDCl_3$): δ 8.27 (d, 1H, J = 4.4 Hz), 8.10 (d, 1H, J = 7.2 Hz), 7.91 (d, 2H, J = 8.7 Hz), 7.87 (d, 1H, J = 4.4 Hz), 7.85 (s, 1H), 7.76 (d, 1H, J = 7.2 Hz), 7.31 (dd, 4H, J = 8.7, 7.2 Hz), 7.21–7.19 (m, 6H), 7.10 (t, 2H, J = 7.2 Hz); ^{13}C NMR (100 MHz, $CDCl_3$): δ 153.8, 152.6, 151.1, 150.4, 148.8, 147.2, 139.0, 135.4, 135.3, 130.1, 129.6, 129.5, 128.2, 128.1, 126.6, 125.2, 123.8, 123.2, 122.3, 114.2, 113.4; FT-IR (neat): 3036, 2223, 1590, 1569, 1537, 1487, 1434, 1327, 1273, 1196, 1112, 815, 757, 697, 609, 510 cm^{-1}; HRMS (ESI-TOF): calcd. for $C_{32}H_{20}N_5S_2$ $[M+H]^+$ 538.1160, found 538.1140.

4.3.5. Compound **E10**

Black solid; yield 30%; ^{1}H NMR (400 MHz, $CDCl_3$): δ 7.68 (s, 1H), 7.54 (d, 1H, J = 3.9 Hz), 7.52 (s, 1H), 7.49 (d, 2H, J = 8.7 Hz), 7.33 (s, 1H), 7.28 (dd, 4H, J = 8.7, 7.3 Hz), 7.21 (d, 1H, J = 3.9 Hz), 7.13 (d, 4H, J = 8.7 Hz), 7.09–7.04 (m, 4H), 1.85 (s, 9H); ^{13}C NMR (100 MHz, $CDCl_3$): δ 151.8, 149.5, 147.7, 147.3, 146.2, 144.4, 143.1, 140.7, 132.3, 130.8, 129.4, 128.9, 126.4, 124.7, 123.4, 123.3, 123.2, 119.8, 115.1, 114.8, 114.3, 114.0, 109.8, 73.8, 58.6, 30.8; FT-IR (neat): 3024, 2218, 1590, 1570, 1517, 1463, 1417, 1372, 1347, 1282, 1232, 1063, 785, 752, 725, 694, 603, 509 cm^{-1}; HRMS (ESI-TOF): calcd. for $C_{38}H_{29}N_4S_3$ $[M+H]^+$ 637.1554, found 637.1493.

4.3.6. Compound **E11**

Black solid; yield 27%; ^{1}H NMR (400 MHz, DMSO-d_6): δ 8.32 (s, 1H), 7.85 (s, 1H), 7.80 (d, 1H, J = 3.9 Hz), 7.74–7.59 (m, 6H), 7.31 (dd, 4H, J = 8.2, 7.7 Hz), 7.08–7.03 (m, 6H), 6.98 (d, 2H, J = 8.7 Hz), 1.81 (s, 9H); ^{13}C NMR (100 MHz, DMSO-d_6): δ 162.7, 146.8, 146.7, 146.5, 145.0, 143.0, 142.8, 141.9, 139.8, 133.1, 131.0, 129.5, 128.8, 126.3, 124.1, 123.9, 123.3, 123.1, 117.0, 116.7, 114.1, 114.0, 110.7, 99.8, 58.4, 30.1; FT-IR (neat): 3183, 2205, 1685, 1574, 1519, 1494, 1419, 1368, 1284, 1094, 941, 797, 754, 697, 611, 509 cm^{-1}; HRMS (ESI-TOF): calcd. for $C_{38}H_{31}N_4OS_3$ $[M+H]^+$ 655.1660, found 655.1636.

4.3.7. Compound **E13**

Dark red solid; yield 22%; Mp 193–197 °C; ^{1}H NMR (400 MHz, $CDCl_3$) δ 7.74 (s, 1H), 7.63 (d, 1H, J = 3.9 Hz), 7.55 (d, 2H, J = 8.7 Hz), 7.39 (d, 1H, J = 3.8 Hz), 7.26 (d, 1H, J = 3.9 Hz), 7.20 (d, 1H, J = 3.8 Hz), 6.94 (d, 2H, J = 8.7 Hz), 3.86 (s, 3H); ^{13}C NMR (100 MHz, $CDCl_3$) δ 160.3, 149.9, 149.7, 147.9, 139.9, 133.2, 128.4, 127.3, 126.1, 124.1, 123.5, 114.7, 114.3, 113.5, 75.9, 55.4; FT-IR (neat) 2936, 2218, 1603, 1570, 1508, 1488, 1428, 1294, 1230, 1175, 1145, 1059, 1030, 932, 843, 813, 799, 788, 604, 495 cm^{-1}; HRMS (ESI-TOF); calcd. for $C_{19}H_{13}N_2OS_2$ $[M+H]^+$ 349.0469, found 349.0435.

4.3.8. Compound **E17**

Black solid; yield 34%; Mp 289–291 °C; ^{1}H NMR (400 MHz, $CDCl_3$): δ 7.71 (s, 1H), 7.58–7.56 (m, 3H), 7.53 (s, 1H), 7.33 (s, 1H), 7.24 (d, 1H, J = 3.9 Hz), 6.95 (d, 2H, J = 8.7 Hz), 3.86 (s, 3H), 1.87 (s, 9H); ^{13}C NMR (100 MHz, $CDCl_3$): δ 159.6, 151.9, 149.6, 146.2, 144.4, 143.0, 140.7, 132.4, 130.7, 128.0, 127.0, 123.2, 119.8, 115.0, 114.8, 114.5, 114.4, 114.0, 109.8, 73.9, 58.6, 55.4, 30.8; FT-IR (neat): 2926, 2212, 1568, 1510, 1460, 1413, 1370, 1342, 1295, 1234, 1177, 1094, 1065, 824, 803, 693, 519 cm^{-1}; HRMS (ESI-TOF): calcd. for $C_{27}H_{22}N_3OS_3$ $[M+H]^+$ 500.0925, found 500.0891.

4.3.9. Compound **E18**

Black solid; yield 11%; ^{1}H NMR (400 MHz, DMSO-d_6): δ 8.31 (s, 1H), 7.84 (s, 1H), 7.80 (d, 1H, J = 3.8 Hz), 7.69–7.57 (m, 6H), 6.98 (d, 2H, J = 8.7 Hz), 3.79 (s, 3H), 1.82 (s, 9H); ^{13}C NMR (100 MHz, DMSO-d_6): δ 162.7, 158.9, 146.6, 145.0, 143.0, 142.6, 142.1, 139.8, 133.1, 130.8, 127.4, 126.5, 123.8, 117.0, 116.7, 114.5, 114.1, 113.6, 110.5, 99.8, 58.4, 55.2, 30.2; FT-IR (neat): 3137, 2208, 1683, 1575, 1518, 1466, 1418, 1369, 1288, 1249, 1233, 1176, 1082, 1056, 798, 752, 684 cm^{-1}; HRMS (ESI-TOF): calcd. for $C_{27}H_{24}N_3O_2S_3$ $[M+H]^+$ 518.1031, found 518.1006.

4.4. Synthesis of compound **E8**

A solution of compound **E6** (40.0 mg, 0.0820 mmol, 1.00 equiv.), cyanoacetamide (**D2**) (13.8 mg, 0.164 mmol, 2.00 equiv.), and piperidine (0.0410 mmol, 4.00 μL, 0.500 equiv.) in a mixture of dichloromethane (1.00 mL) and acetonitrile (0.500 mL) was stirred at 40 °C for 6.5 h under argon. The mixture was poured into saturated aq. NH_4Cl and the aqueous layer was extracted with three portions of dichloromethane. The organic layer was dried over $MgSO_4$ and evaporated *in vacuo*. The residue was purified by column chromatography on silica gel with chloroform to give the product **E8** (24.0 mg, 0.0432 mmol, 53%).

Red solid; Mp 273–274 °C; ^{1}H NMR (400 MHz, DMSO-d_6): δ 8.41 (s, 1H), 8.31 (d, 1H, J = 7.2 Hz), 8.27 (d, 1H, J = 4.3 Hz), 7.99–7.92 (m, 4H), 7.82 (br-s, 1H), 7.71 (br-s, 1H), 7.36 (dd, 4H, J = 8.3, 7.8 Hz), 7.12–7.07 (m, 8H); ^{13}C NMR (100 MHz, DMSO-d_6): δ 162.6, 153.0, 151.8, 147.8, 146.7, 146.1, 143.2, 138.2, 136.7, 133.0, 130.2, 129.7, 127.7, 127.6, 127.1, 124.6, 123.7, 123.3, 121.9, 116.8, 101.8; FT-IR (neat): 3172, 2209, 1679, 1576, 1512, 1486, 1441, 1381, 1330, 1286, 1225, 902, 813, 754, 698, 511 cm^{-1}; HRMS (ESI-TOF): calcd. for $C_{32}H_{22}N_5OS_2$ $[M+H]^+$ 556.1266, found 556.1218.

4.5. Synthesis of compound **E4**

A solution of compound **E2** (10.0 mg, 0.0229 mmol, 1.00 equiv.), barbituric acid (2.9 mg, 0.023 mmol, 1.0 equiv.), and acetic anhydride (11.3 μL, 0.115 mmol, 5.00 equiv.) in acetic acid (1.00 mL) was refluxed for 3.5 h. The mixture was evaporated *in vacuo*. The residue was purified by column chromatography on silica gel with chloroform to give compound **E4** (11.9 mg, 0.0218 mmol, 95%).

Dark red solid; Mp 291–293 °C; ^{1}H NMR (400 MHz, DMSO-d_6): δ 11.25 (s, 1H), 11.24 (s, 1H), 8.46 (s, 1H), 8.14 (d, 1H, J = 3.9 Hz), 7.67 (d, 1H, J = 3.9 Hz), 7.65–7.61 (m, 3H), 7.50 (d, 1H, J = 3.9 Hz), 7.34 (dd, 4H, J = 8.2, 7.8 Hz), 7.12–7.07 (m, 6H), 6.96 (d, 2H, J = 8.7 Hz); ^{13}C NMR (100 MHz, DMSO-d_6): δ 163.4, 163.3, 151.1, 150.3, 147.6, 147.4, 146.6, 145.8, 145.2, 134.7, 133.6, 129.7, 128.6, 126.7, 126.3, 124.6, 124.4, 123.7, 122.3, 110.0; FT-IR (solid): 3203, 3068, 2924, 2853, 2382, 1740, 1660, 1568, 1487, 1398, 1264, 1199, 1093, 795, 754, 697, 621, 545, 517 cm^{-1}; HRMS (ESI-TOF): calcd. for $C_{31}H_{22}N_3O_3S_2$ $[M+H]^+$ 548.1103, found 548.1097.

4.6. Preparation of tau protein (3R MBD)

The His-tagged 3R MBD of human brain tau expressed in *E. coli* BL21(DE3) was kindly provided by Professor T. Ishida (Osaka Univ. of Pharmaceutical Sciences) [25]. Bacterial culture was grown with shaking at 37 °C until the OD_{600} reached 0.5. The expression of 3R MBD was induced by adding IPTG. After shaking for 4 h at 37 °C, bacterial cells were collected by centrifuge. Bacterial pellets were resuspended in 50 mM Tris–HCl, pH 7.6, 50 mM NaCl and sonicated. Then the homogenates were centrifuged and the supernatants were purified on the Ni-chelating chromatography using Ni Sepharose 6 Fast Flow (GE Healthcare, Amersham, UK). 3R MBD was eluted with 50 mM Tris–HCl, pH 7.6, 500 mM NaCl, and 100 mM imidazole. The eluted solution containing 3R MBD was dialyzed against 100 mM ammonium acetate and freeze-dried. The purified tau protein (3R MBD) was stored at −30 °C until use.

4.7. Inhibition of Aβ1–42 aggregation [23,24]

Aβ1–42 peptide (Peptide Institute, Inc.) was dissolved in 0.1% aq. NH_3 and diluted to 20 μM in PBS (solution **A**). The synthesized

compound dissolved in DMSO was diluted 50-fold with PBS (solution **B**). ThT (Sigma–Aldrich Corporation, Japan) dissolved in water was diluted by 6 μM in 100 mM Tris–glycine, pH 8.5 (solution **C**). Solutions **A** and **B** were mixed with equal volume and incubated for 24 h at 37 °C without exposure to light. The compound concentrations were 1, 3, and 10 μM in the assay shown in Table 3, and 0.1, 0.3, 1, 3, and 10 μM in the assay shown in Table 4. At the end of the incubations, the fluorescence intensity of the sample solution was measured as the background. Then solution **C** was added into the sample solution at an equal volume and ThT fluorescence intensity was measured for the quantitative assessment of Aβ1–42 peptide aggregation. Fluorescence intensity was measured via excitation at 440 nm and emission at 486 nm using a Perkin Elmer AROV Wallac1420. The IC_{50}s shown in Table 4 were determined by the averages of two independent experiments.

4.8. Inhibition of tau aggregation [25]

The synthesized compound was dissolved in DMSO, 10 μM tau (3R-MBD) and 10 μM heparin (Sigma–Aldrich Corporation, Japan) in 50 mM Tris–HCl, pH 7.6 and was incubated at 37 °C for 16 h without exposure to light. The compound concentrations were 0.1–10 μM. Following incubation, the fluorescence intensity of the sample solution was measured as the background. Then 10 μM ThT solution was added into each sample solution and ThT fluorescence intensity was measured for quantitative assessment of tau protein aggregation. Fluorescence intensity was measured via excitation at 440 nm and emission at 486 nm using a Perkin Elmer AROV Wallac1420.

Appendix A. Supplementary data

Supplementary data associated with this article can be found in the online version, at http://dx.doi.org/10.1016/j.ejmech.2014.07.095. These data include MOL files and InChiKeys of the most important compounds described in this article.

References

[1] K.R. Brunden, J.Q. Trojanowski, V.M.Y. Lee, Advances in tau-focused drug discovery for Alzheimer's disease and related tauopathies, Nat. Rev. Drug Discov. 8 (2009) 783–793.

[2] Y.D. Huang, L. Mucke, Alzheimer mechanisms and therapeutic strategies, Cell 148 (2012) 1204–1222.

[3] R. Christiane, Alzheimer's disease and the amyloid cascade hypothesis: a critical review, Int. J. Alzheimers Dis. 2012 (2012) 1–11.

[4] S. Taniguchi, N. Suzuki, M. Masuda, S. Hisanaga, T. Iwatsubo, M. Goedert, M. Hasegawa, Inhibition of heparin-induced tau filament formation by phenothiazines, polyphenols, and porphyrins, J. Biol. Chem. 280 (2005) 7614–7623.

[5] C.M. Wischik, P.C. Edwards, R.Y.K. Lai, M. Roth, C.R. Harrington, Selective inhibition of Alzheimer disease-like tau aggregation by phenothiazines, Proc. Natl. Acad. Sci. U. S. A. 93 (1996) 11213–11218.

[6] M. Catto, A.A. Berezin, D. Lo Re, G. Loizou, M. Demetriades, A. De Stradis, F. Campagna, P.A. Koutentis, A. Carotti, Design, synthesis and biological evaluation of benzo[*e*][1,2,4]triazin-7(1*H*)-one and [1,2,4]-triazino[5,6,1-*jk*] carbazol-6-one derivatives as dual inhibitors of beta-amyloid aggregation and acetyl/butyryl cholinesterase, Eur. J. Med. Chem. 58 (2012) 84–97.

[7] S.-Y. Li, X.-B. Wang, S.-S. Xie, N. Jiang, K.D.G. Wang, H.-Q. Yao, H.-B. Sun, L.-Y. Kong, Multifunctional tacrine–flavonoid hybrids with cholinergic, β-amyloid-reducing, and metal chelating properties for the treatment of Alzheimer's disease, Eur. J. Med. Chem. 69 (2013) 632–646.

[8] K.R.J. Thomas, Y.C. Hsu, J.T. Lin, K.M. Lee, K.C. Ho, C.H. Lai, Y.M. Cheng, P.T. Chou, 2,3-Disubstituted thiophene-based organic dyes for solar cells, Chem. Mater. 20 (2008) 1830–1840.

[9] Y.S. Yen, Y.C. Hsu, J.T. Lin, C.W. Chang, C.P. Hsu, D.J. Yin, Pyrrole-based organic dyes for dye-sensitized solar cells, J. Phys. Chem. C 112 (2008) 12557–12567.

[10] Y.J. Chang, T.J. Chow, Dye-sensitized solar cell utilizing organic dyads containing triarylene conjugates, Tetrahedron 65 (2009) 4726–4734.

[11] S.J. Moon, J.H. Yum, R. Humphry-Baker, K.M. Karlsson, D.P. Hagberg, T. Marinado, A. Hagfeldt, L.C. Sun, M. Gratzel, M.K. Nazeeruddin, Highly efficient organic sensitizers for solid-state dye-sensitized solar cells, J. Phys. Chem. C 113 (2009) 16816–16820.

[12] S. Fuse, H. Yoshida, T. Takahashi, An iterative approach to the synthesis of thiophene-based organic dyes, Tetrahedron Lett. 53 (2012) 3288–3291.

[13] S. Fuse, H. Tago, M.M. Maitani, Y. Wada, T. Takahashi, Sequential coupling approach to the synthesis of nickel(II) complexes with *N*-aryl-2-amino phenolates, ACS Combi. Sci. 14 (2012) 545–550.

[14] S. Fuse, K. Inaba, M. Takagi, M. Tanaka, T. Hirokawa, K. Johmoto, H. Uekusa, K. Shin-Ya, T. Takahashi, T. Doi, Design and synthesis of 2-phenyl-1,4-dioxaspiro[4.5]deca-6,9-dien-8-ones as potential anticancer agents starting from cytotoxic spiromamakone A, Eur. J. Med. Chem. 66 (2013) 180–184.

[15] S. Fuse, S. Sugiyama, M.M. Maitani, Y. Wada, Y. Ogomi, S. Hayase, R. Katoh, T. Kaiho, T. Takahashi, Elucidating the structure–property relationship of donor-π-acceptor dyes for DSSCs through rapid library synthesis via a one-pot procedure, Chem. Eur. J. Early View 10.1002/chem.201402093.

[16] M. Gruttadauria, L.A. Bivona, P. Lo Meo, S. Riela, R. Noto, Sequential Suzuki/asymmetric aldol and Suzuki/Knoevenagel reactions under aqueous conditions, Eur. J. Org. Chem. 2012 (2012) 2635–2642.

[17] L. Malatesta, M. Angoletta, Palladium(0) compounds. Part II. Compounds with triarylphosphines, triaryl phosphites, and triarylarsines, J. Chem. Soc. (1957) 1186–1188.

[18] Y. Takahashi, T. Ito, S. Sakai, Y. Ishii, A novel palladium(0) complex; bis(dibenzylideneacetone)palladium(0), J. Chem. Soc. Chem. Commun. (1970) 1065–1066.

[19] M. Kranenburg, Y.E.M. Vanderburgt, P.C.J. Kamer, P. Vanleeuwen, K. Goubitz, J. Fraanje, New diphosphine ligands based on heterocyclic aromatics inducing very high regioselectivity in rhodium-catalyzed hydroformylation – effect of the bite angle, Organometallics 14 (1995) 3081–3089.

[20] A.F. Littke, C.Y. Dai, G.C. Fu, Versatile catalysts for the Suzuki cross-coupling of arylboronic acids with aryl and vinyl halides and triflates under mild conditions, J. Am. Chem. Soc. 122 (2000) 4020–4028.

[21] M.D. Obushak, V.S. Matiychuk, R.Z. Lytvyn, Synthesis and reactions of 5-aryl-2-thiophenecarbaldehydes, Chem. Heterocycl. Compd. 44 (2008) 936–940.

[22] C. Nitsche, C. Steuer, C.D. Klein, Arylcyanoacrylamides as inhibitors of the Dengue and West Nile virus proteases, Bioorg. Med. Chem. 19 (2011) 7318–7337.

[23] H. Levine, Thioflavine-T interaction with synthetic Alzheimer's disease β-amyloid peptides – detection of amyloid aggregation in solution, Protein Sci. 2 (1993) 404–410.

[24] S.A. Hudson, H. Ecroyd, T.W. Kee, J.A. Carver, The thioflavin T fluorescence assay for amyloid fibril detection can be biased by the presence of exogenous compounds, FEBS J. 276 (2009) 5960–5972.

[25] K. Okuyama, C. Nishiura, F. Mizushima, K. Minoura, M. Sumida, T. Taniguchi, K. Tomoo, T. Ishida, Linkage-dependent contribution of repeat peptides to self-aggregation of three- or four-repeat microtubule-binding domains in tau protein, FEBS J. 275 (2008) 1529–1539.

[26] K. Amro, J. Daniel, G. Clermont, T. Bsaibess, M. Pucheault, E. Genin, M. Vaultier, M. Blanchard-Desce, A new route towards fluorescent organic nanoparticles with red-shifted emission and increased colloidal stability, Tetrahedron 70 (2014) 1903–1909.

[27] K. Do, C. Kim, K. Song, S.J. Yun, J.K. Lee, J. Ko, Efficient planar organic semiconductors containing fused triphenylamine for solution processed small molecule organic solar cells, Sol. Energy Mater. Sol. Cells 115 (2013) 52–57.

[28] E. Genin, Z. Gao, J.A. Varela, J. Daniel, T. Bsaibess, I. Gosse, L. Groc, L. Cognet, M. Blanchard-Desce, "Hyper-bright" near-infrared emitting fluorescent organic nanoparticles for single particle tracking, Adv. Mater. 26 (2014) 2258–2261.

[29] A. Gupta, A. Ali, A. Bilic, M. Gao, K. Hegedus, B. Singh, S.E. Watkins, G.J. Wilson, U. Bach, R.A. Evans, Absorption enhancement of oligothiophene dyes through the use of a cyanopyridone acceptor group in solution-processed organic solar cells, Chem. Commun. 48 (2012) 1889–1891.

[30] T. Khanasa, N. Jantasing, S. Morada, N. Leesakul, R. Tarsang, S. Namuangruk, T. Kaewin, S. Jungsuttiwong, T. Sudyoadsuk, V. Promarak, Synthesis and characterization of 2D-D-π-A-type organic dyes bearing bis(3,6-di-tert-butylcarbazol-9-ylphenyl)aniline as donor moiety for dye-sensitized solar cells, Eur. J. Org. Chem. 2013 (2013) 2608–2620.

[31] M. Velusamy, K.R.J. Thomas, J.T. Lin, Y.-C. Hsu, K.-C. Ho, Organic dyes incorporating low-band-gap chromophores for dye-sensitized solar cells, Org. Lett. 7 (2005) 1899–1902.

[32] W. Zhu, Y. Wu, S. Wang, W. Li, X. Li, J. Chen, Z.-S. Wang, H. Tian, Organic D-A-π-A solar cell sensitizers with improved stability and spectral response, Adv. Funct. Mater. 21 (2011) 756–763.